AGU PUBLICATIONS

Geophysical Research Letters

RESEARCH LETTER
10.1002/2015GL064914

Key Points:
- Extremes warm ~2°C more than mean
- Order of magnitude recurrence changes
- RCMs capture dynamics

Supporting Information:
- Supporting Information S1

Correspondence to:
R. M. Horton,
rh142@columbia.edu

Citation:
Horton, R. M., E. D. Coffel, J. M. Winter, and D. A. Bader (2015), Projected changes in extreme temperature events based on the NARCCAP model suite, *Geophys. Res. Lett.*, *42*, 7722–7731, doi:10.1002/2015GL064914.

Received 19 JUN 2015
Accepted 11 AUG 2015
Accepted article online 14 AUG 2015
Published online 16 SEP 2015

Projected changes in extreme temperature events based on the NARCCAP model suite

Radley M. Horton[1,2], Ethan D. Coffel[2,3], Jonathan M. Winter[4], and Daniel A. Bader[1,2]

[1]Center for Climate Systems Research, Columbia University, New York, New York, USA, [2]NASA Goddard Institute for Space Studies, New York, New York, USA, [3]Department of Earth and Environmental Sciences, Columbia University, New York, New York, USA, [4]Department of Geography and Department of Earth Sciences, Dartmouth College, Hanover, New Hampshire, USA

Abstract Once-per-year (annual) maximum temperature extremes in North American Regional Climate Change Assessment Program (NARCCAP) models are projected to increase more (less) than mean daily maximum summer temperatures over much of the eastern (western) United States. In contrast, the models almost everywhere project greater warming of once-per-year minimum temperatures as compared to mean daily minimum winter temperatures. Under projected changes associated with extremes of the temperature distribution, Baltimore's maximum temperature that was met or exceeded once per year historically is projected to occur 17 times per season by midcentury, a 28% increase relative to projections based on summer mean daily maximum temperature change. Under the same approach, historical once-per-year cold events in Baltimore are projected to occur once per decade. The models are generally able to capture observed geopotential height anomalies associated with temperature extremes in two subregions. Projected changes in extreme temperature events cannot be explained by geopotential height anomalies or lower boundary conditions as reflected by soil moisture anomalies or snow water equivalent.

1. Introduction

Temperature extremes, both high and low, have disproportionate impacts on society [*Handmer et al.*, 2012]. Extreme heat is the leading weather-related cause of death in the United States [*National Oceanic and Atmospheric Administration*, 2015], reduces agricultural yields [*Schlenker and Roberts*, 2009], and damages and disrupts infrastructure [*Sathaye et al.*, 2013; *Meyer et al.*, 2010; *Coffel and Horton*, 2015]. Extreme cold events are associated with ecosystem impacts [*Ammunét et al.*, 2012], elevated human mortality [*Kalkstein and Greene*, 1997], and damage to infrastructure [*Horton et al.*, 2010]. Because many human and natural systems are highly sensitive to temperature extremes, projections of how these extremes may change are particularly important.

Recent years have seen an expansion beyond exploring mean changes to, increasingly, changes in extreme events [*Jones et al.*, 2015; *Handmer et al.*, 2012; *Walsh et al.*, 2014]. Globally, observational analyses have reported fast warming of both cold and warm extremes, with the rate of warming for cold extremes exceeding the rate of warming for hot extremes over much of the globe [*Hartmann et al.*, 2013]. While some evidence does exist that hot extremes have been increasing in the recent past in the U.S. [*Meehl et al.*, 2009], changes in high-temperature extremes over the observational record have been shown to be largely insignificant across much of the country [*Alexander et al.*, 2006]. This lack of trend in hot extremes is consistent with the lack of substantial mean changes over parts of the nation, including "warming holes" found over the southeastern and central U.S. [*Pan et al.*, 2004; *Kunkel et al.*, 2006; *Meehl et al.*, 2012].

Modeling studies have projected faster warming of extremes than means globally [*Orlowsky and Seneviratne*, 2011; *Schär et al.*, 2004]. *Kharin et al.* [2007] projected that warming of extreme minimum temperatures might exceed that of extreme maximum temperatures by one third. Regional modeling studies have also identified a tendency for some extremes to increase more rapidly than mean conditions [*Kjellström et al.*, 2007]. *Ballester et al.* [2009] found increases in temperature variability linked to summers warming more than winters, rather than changes in the statistics of daily/subseasonal extremes.

Statistical downscaling is increasingly used to project changes in extremes at the regional level. In the northeast U.S., for example, *Ahmed et al.* [2013] and *Ning et al.* [2015] found that statistical downscaling approaches could be used to simulate ecologically relevant temperature-related metrics, such as growing

Table 1. GCM/RCM (Column/Row) Combinations Used in Analysis[a]

	CCSM	CGCM3	GFDL	HADCM3
CRCM		T, Z, M, and S	T, Z, M, and S	
ECP2			T, Z, M, and S	
HRM3			T, Z, and M	T and Z
MM5I	T, Z, and M			T, Z, and M
RCM3		T, Z, M, and S	T, Z, and S	
WRFG	T, Z, M, and S	T, Z, and M		

[a] "T" means the combination was used for temperature, "Z" for 500 hPa geopotential height, "M" for soil moisture, and "S" for snow water equivalent.

season length and 10th and 90th percentiles of daily temperature. We here add to the existing downscaling research by using regional climate models to evaluate projections of how rarer once-per-year (annual) temperature extremes change relative to seasonal average changes for the same metric, i.e., maximum temperatures in summer and minimum temperatures in winter. By using dynamical downscaling as opposed to statistical downscaling, we are able to explore potential non-stationarity in the circulation and lower boundary condition drivers of once-per-year temperature changes.

2. Methods

We use regional climate model (RCM) simulations at 50 km^2 resolution from the North American Regional Climate Change Assessment Program (NARCCAP) [*Mearns et al.*, 2012; *Mearns and Gutowski*, 2009] to assess how once-per-year (annual) maximum and minimum temperatures (TXx and TNn) are projected to change by midcentury (2051–2069) under the Special Report on Emissions Scenarios A2 emissions scenario [*Nakicenovic et al.*, 2000]. NARCCAP has been evaluated against observations for a variety of metrics and domains, including daily temperature trends in the U.S. [*Bukovsky*, 2012] and mean seasonal surface temperature and precipitation over the southeast [*Sobolowski and Pavelsky*, 2012], and the North American monsoon [*Bukovsky et al.*, 2013]. *Mearns et al.* [2015] document a range of studies that have applied NARCCAP results to climate change impacts and adaptation assessments.

NARCCAP uses four general circulation models (GCMs) to drive six RCMs. We use RCMs because their relatively high resolution has been shown to improve the simulation of climate extremes relative to global models [*Caldwell et al.*, 2009]. The ability of NARCCAP simulations to reproduce the historical climatology of extreme events was evaluated by comparing RCM simulations to North American Regional Reanalysis (NARR) [*Mesinger et al.*, 2006]. Projections are based on outputs from 11 GCM/RCM combinations for the 2051–2069 period relative to the hindcast period of 1981–1998. The GCM/RCM combinations used are shown in Table 1. Results are presented as maps for the full U.S., and additional analyses are presented for two subregions, one in the northeast (between 39–41°N and 76–80°W) and one in the southwest (between 34–36°N and 108–112°W).

3. Results

3.1. Heat Events

Figures 1a and 1b show increases in both once-per-year maximum temperature (TXx) and mean summer daily maximum temperature (Tx). Significant changes are defined as a change of greater than 2 standard deviations calculated from daily data for June, July, and August (JJA) over the historical period (1981–1998) and are denoted by stippling in figures. Figure 1e shows that TXx changes are greater than Tx changes over much of the eastern U.S., with nearly all models showing TXx rising faster than Tx for this region (Figure 2a). Over the north central and northeast U.S. the NARCCAP models project TXx increases of 4–4.5°C by 2051–2069 relative to 1981–1998. During the same period, Tx is projected to increase by only 3–3.5°C. In the western half of the U.S., however, the NARCCAP models project that mean daily maximum temperatures increase slightly faster than extremes (Figure 1e).

We investigate several possible mechanisms for these patterns. Dynamical drivers associated with extreme heat events include positive geopotential height anomalies throughout the troposphere and low-level southerly winds [*Meehl and Tebaldi*, 2004]. Many observational and modeling studies have also identified negative soil moisture anomalies as an important source of surface heating through enhanced sensible heat

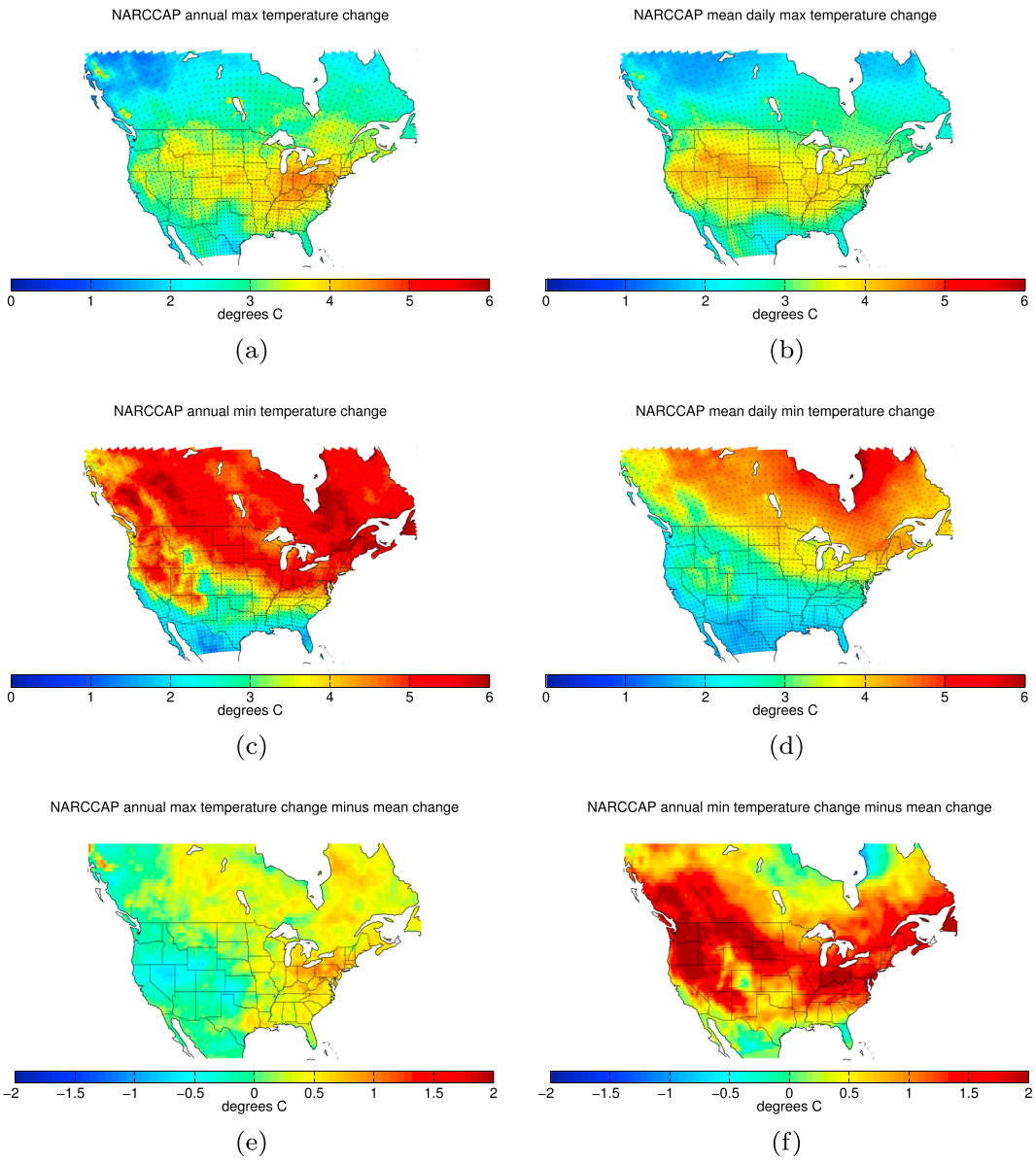

Figure 1. (a) NARCCAP multimodel mean change in June, July, and August (JJA) annual maximum temperature (TXx) in 2051–2069 relative to 1981–1998. (b) Same as Figure 1a but for mean JJA daily maximum temperature (Tx). (c) Same as Figure 1a but for December, January, and February (DJF) annual minimum temperature (TNn). (d) Same as Figure 1b but for mean DJF daily minimum temperature (Tn). (e) Change in TXx minus change in Tx (Figure 1a minus Figure 1b). (f) Change in TNn minus change in Tn (Figure 1c minus Figure 1d).

flux [*Diffenbaugh and Ashfaq*, 2010; *Hirschi et al.*, 2010]. However, soil moisture is difficult to compare between models due to different definitions of the soil moisture variable [*Cook et al.*, 2015]. Here we find that the soil moisture anomalies within the NARCCAP modeling suite are not consistent with NARR soil moisture anomalies for TXx days (not shown), so we instead focus our analysis on geopotential heights.

We first investigate whether the NARCCAP models capture observed patterns in 500 hPa geopotential height anomalies during extreme heat events. Dynamic drivers of extreme temperature events are assessed in the two chosen subregions in the northeast and southwest. Within these regions, we composite domain-wide 500 hPa geopotential height anomalies and vertical temperature profiles for the 1 d/yr with the highest maximum temperature averaged over the target region in both the NARR and the NARCCAP models.

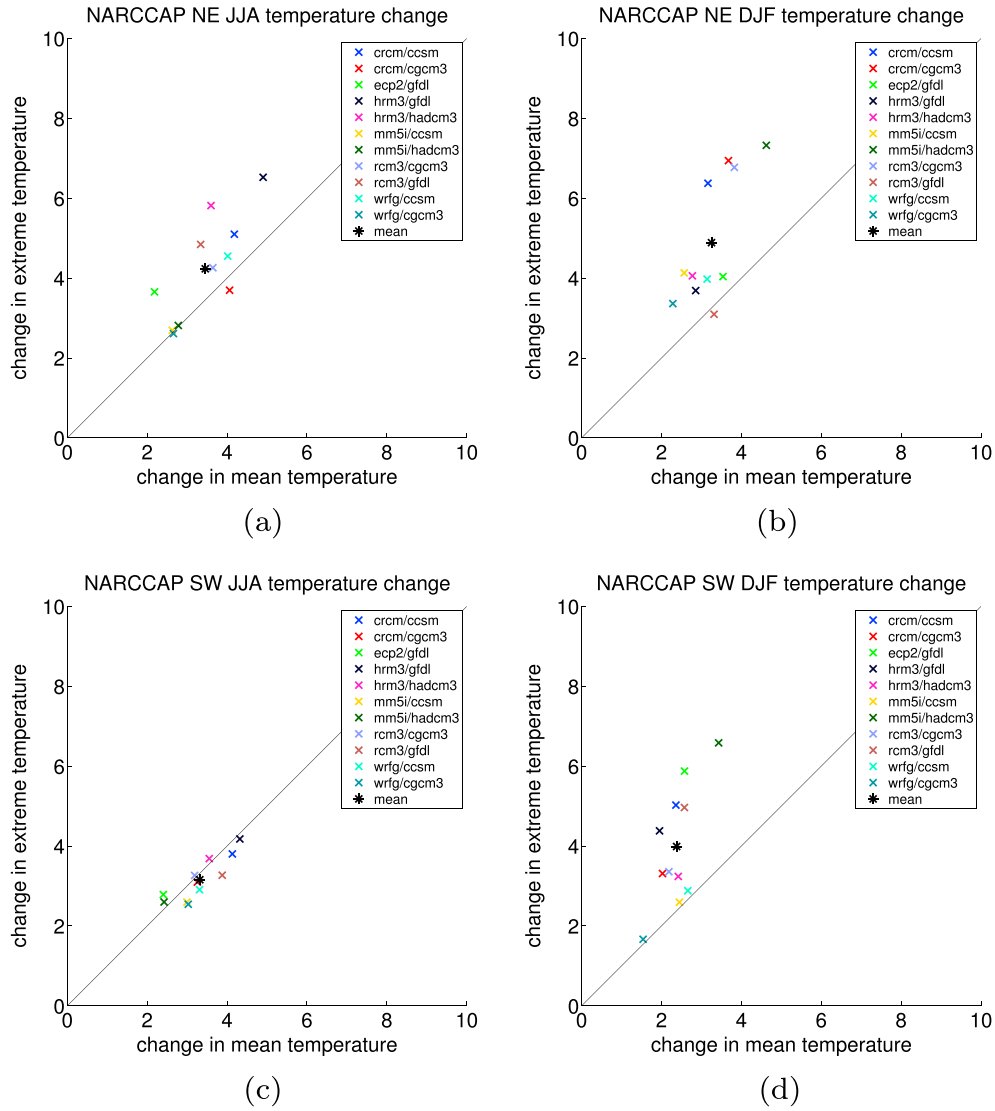

Figure 2. Comparison of changes (2051–2069 minus 1981–1999) in (a) JJA TXx and Tx for the northeast. (b) Same as Figure 2a but for TNn and Tn. (c) Same as Figure 2a but for the southwest. (d) Same as Figure 2b but for the southwest. The black line represents slope one.

NARCCAP represents 500 hPa geopotential height anomalies well as compared with NARR; Figures 3a and 3c show the NARR and NARCCAP multimodel mean 500 hPa geopotential height anomalies for TXx days in the northeast region (and Figures 4a and 4c show the same for the southwest). On the hottest days, 500 hPa geopotential height anomalies of approximately 50–70 m and 80–100 m are present in NARCCAP and NARR, respectively. Both the NARR and NARCCAP positive anomalies are generally centered over the area with extreme high temperatures. In the northeast, the NARR geopotential height anomaly has a sharper gradient and expands farther north than the NARCCAP anomaly. In the southwest region, both the NARR data and NARCCAP models contain a ridge in the region of high temperatures, although the NARR anomaly has a larger magnitude. In both NARR and NARCCAP the TXx anomalies relative to Tx persist in both regions up to 500 hPa (supporting information Figures S1a and S2a). The positive 500 hPa geopotential height anomalies on the hottest days in both NARR and NARCCAP are consistent with the fact that 500 hPa height anomalies are related to the integral of temperature anomalies between that level and the surface.

We find no significant future intensification of 500 hPa geopotential height anomalies on TXx (annual maximum temperature) days relative to summer mean geopotential height in the future, in either region

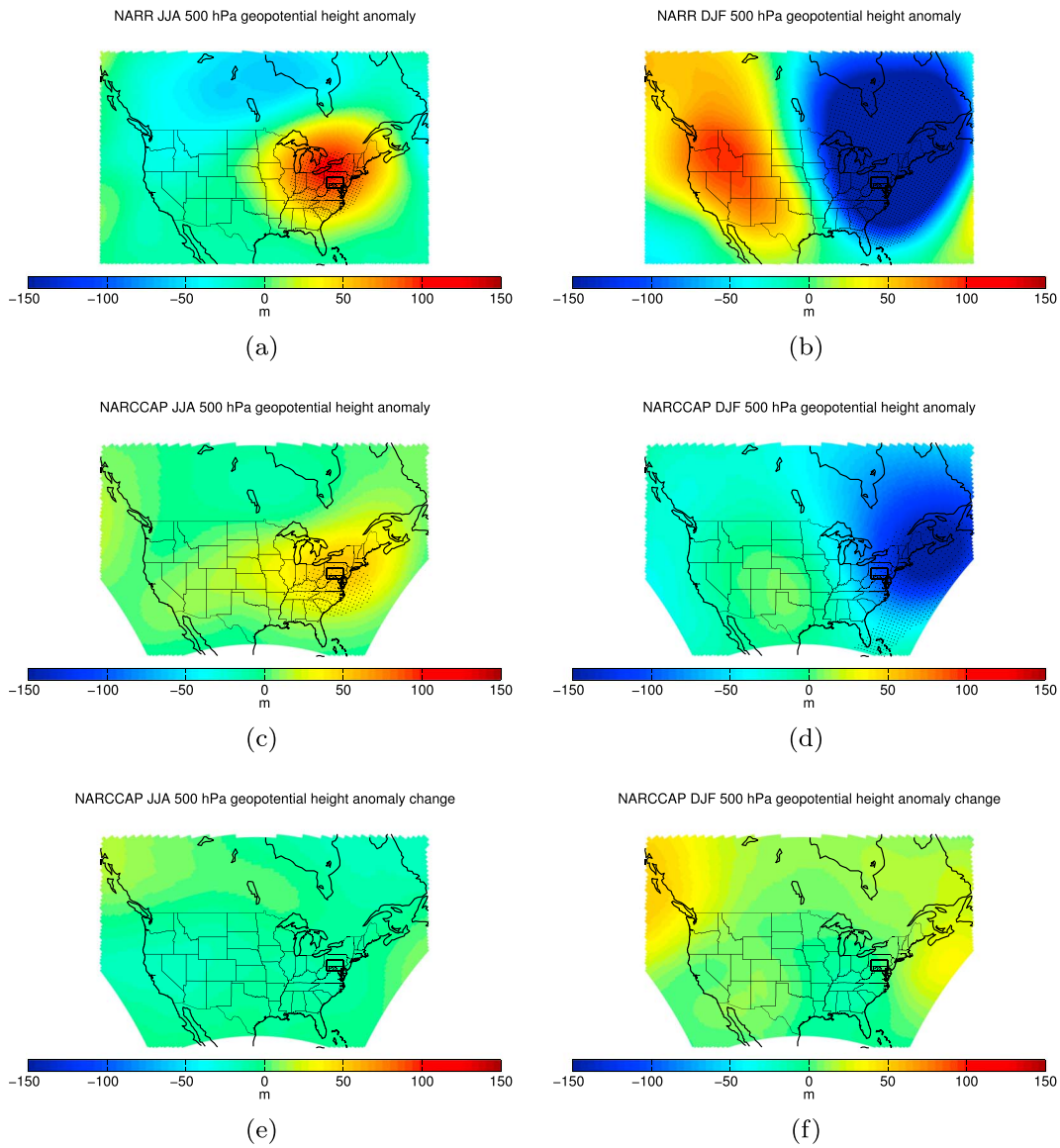

Figure 3. (a) NARR 500 hPa geopotential height anomaly on JJA TXx days during the reference period (1981–1998) in the northeast region (shown by black box). (b) Same as Figure 3a but for DJF TNn. (c) Same as Figure 3a but using the NARCCAP multimodel mean. (d) Same as Figure 3b but using the NARCCAP multimodel mean. (e) Change in NARCCAP 500 hPa geopotential height anomaly on JJA TXx days between the future period (2051–2069) relative to the reference period (1981–1998). (f) Same as Figure 3e but for DJF TNn. Stippling indicates significance at 2 standard deviations above the multimodel mean daily variability.

(Figures 3e and 4e). As shown for the northeast in the supporting information Figure S1b, Tx warming is relatively consistent with height, whereas TXx warming is roughly twice as large at the surface than at 500 hPa. TXx therefore features greater warming than Tx up to about 700 hPa and less warming above 700 hPa, leading to counteracting effects on the future 500 hPa height departure for the TXx case relative to the Tx case. Future work could explore possible drivers in the models of these changing temperature profiles (e.g., vertical mixing) and 500 hPa heights (e.g., changes in pressure driven by shifting weather systems/local dynamics), as well as the consistency of these features across locations and models.

3.2. Cold Events

Changes in once-per-year daily minimum temperatures (TNn) are appreciably larger than changes in winter mean daily minimum temperatures (Tn) over most of the domain, as shown in Figures 1c, 1d, and 1f, with differences peaking at approximately 2°C in parts of the western, midwestern, and northeastern U.S. In nearly

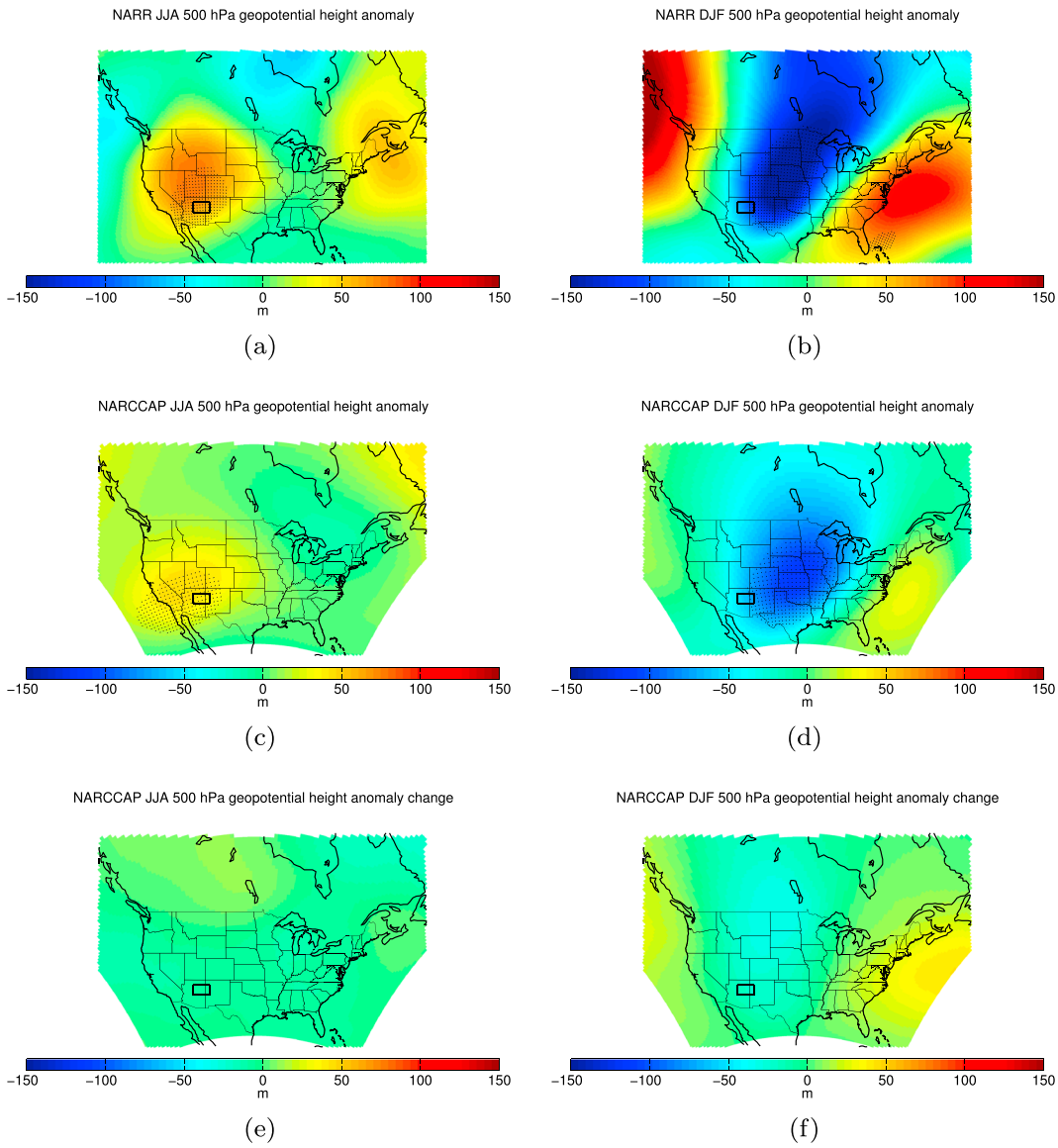

Figure 4. (a) NARR 500 hPa geopotential height anomaly on JJA TXx days during the reference period (1981–1998) in the southwest region (shown by black box). (b) Same as Figure 4a but for DJF TNn. (c) Same as Figure 4a but using the NARCCAP multimodel mean. (d) Same as Figure 4b but using the NARCCAP multimodel mean. (e) Change in NARCCAP 500 hPa geopotential height anomaly on JJA TXx days between the future period (2051–2069) relative to the reference period (1981–1998). (f) Same as Figure 4e but for DJF TNn. Stippling indicates significance at 2 standard deviations above the mean daily variability.

all NARCCAP models the coldest wintertime temperatures are projected to increase more than the mean for most regions of the U.S. (Figures 2b and 2d show results from the northeast and southwest domains, respectively). We see a relatively sharp cutoff line north of which the change in wintertime TNn ranges from 4 to 5°C, as compared with the much smaller change in Tn of 2.5–3°C (Figure 1c and 1d). South of this line, TNn increases by 2–3°C while Tn increases by 2–2.5°C.

To explore possible mechanisms driving these changes, we again look at the 500 hPa geopotential height and vertical temperature profiles, as well as snow cover, which induces albedo and sensible heat flux feedbacks [*Kjellström et al.*, 2007; *Diffenbaugh et al.*, 2005]. In the northeast U.S., *Leathers et al.* [1995] found that maximum and minimum temperatures were 5°C cooler when snow cover exceeded 2.5 cm. Over the Great Plains, *Ellis and Leathers* [1999] reported even larger maximum temperature departures associated with an absence of snow cover, although the effect on nighttime minimum temperatures was muted, at just 1–2°C.

In the northeast, *Bradbury et al.* [2002] link a deep 500 hPa trough near the U.S. East Coast to anomalously cold months and the negative phase of the North Atlantic Oscillation (NAO), through more frequent northerly cold air intrusions associated with enhanced blocking farther east [*Yarnal and Leathers*, 1988]. *Ning and Bradley* [2015] linked both the negative phase of the NAO and the positive phase of the Pacific/North American Pattern to an increasing number of cold nights in the general area of our northeast region, although the relationship was stronger for the 10th percentile cold nights than for the coldest night per year.

As shown in Figures 3b, 3d, 4b, and 4d, we find that days with extreme minimum temperatures in the northeast and southwest are associated with strong and spatially expansive negative 500 hPa geopotential height anomalies (and a deepening of the 500 hPa trough in the northeast, not shown) in both NARR and NARCCAP. For the northeast, this relationship is consistent with the findings of both *Bradbury et al.* [2002] and *Ning and Bradley* [2015] and resembles conditions more likely to occur during the negative phase of the NAO. Generally, the NARCCAP models capture the amplitude and location of the negative anomalies in NARR. However, the NARCCAP negative anomaly corresponding to TNn in the northeast is too small and shifted to the east, and the NARCCAP negative anomaly corresponding to TNn in the southwest is too weak compared to NARR. For both TXx and TNn across the northeast and southwest, the representation of the geopotential height anomalies seems to deteriorate toward the domain edges. For example, the compensating antipodal ridges (i.e., over the east when the southwest is cold and over the west when the northeast is cold) are of insufficient size and amplitude. In both subregions (supporting information Figures S1c and S2c), the negative temperature anomalies on TNn days persist up to (and above) 500 mb, supporting the negative geopotential height anomalies on those days relative to the winter mean. In both regions, the winter minimum profiles also show more stable temperature profiles than are present for the summer maximums, consistent with a more shallow boundary layer and more air inversions.

The large projected increase in TNn as compared with Tn over the Northeast (Figure 1f) is not reflected in the 500 hPa geopotential height levels, which show no significant change in 500 hPa geopotential height anomalies on TNn days (Figure 3f). This is true despite the fact that warming on TNn days exceeds Tn warming from the surface up to 300 mb (supporting information Figure S1d), raising the possibility of some offsetting dynamical effects. Changes in snow water equivalent in the NARCCAP models are also not sufficient to explain the change in winter temperatures (not shown). Over the southwest, Figure 4f shows a moderately large change of up to 25 m in 500 hPa geopotential height anomalies that is spatially similar to and (counterintuitively given the large Tn warming) of the same sign as the 500 hPa geopotential height anomaly for TNn in the NARCCAP historical period. As with the warming of TXx relative to Tx, the negative sign (relative to Tn days) of this 500 hPa geopotential height anomaly can be explained by the fact that although the NARCCAP models project larger warming of TNn relative to Tn near the surface, higher up (800 hPa) there is less warming (supporting information Figure S2d).

4. Projected Changes in Frequency of Temperature Extremes

Our finding that extreme temperatures may warm at a different magnitude than seasonal averages points to the potential for sharply nonlinear changes in the frequency of occurrence of extreme temperatures, with associated potentially nonlinear societal impacts. We explore changes in the frequency of extreme events using the delta method, whereby the amount of warming in all—or a subset—of the RCM distribution is applied to observed historical data. Bias correction such as this is necessary, since the NARCCAP RCMs include biases at local as well as regional scales. Table 2 shows changes in the recurrence frequency of the historical once-per-year hot and cold extremes using warming projected by the NARCCAP models. We choose one city in our northeast and one city in our southwest domains: Baltimore, MD, and Flagstaff, AZ. These results both demonstrate how profoundly the application of seasonal mean changes can impact the frequency of extremes (second column from the right) and that further large changes in frequency can occur when the deltas associated with extremes (as opposed to the seasonal means) are applied to the observed extremes (right column). For example, when the summer mean daily maximum temperature (Tx) changes for the NARCCAP grid box covering Baltimore are applied to Baltimore's observed daily temperature data, the high-temperature extreme that was met or exceeded once per year historically may occur 13 times per season. When the delta associated with the high tail of the distribution analyzed in this paper (TXx) is applied, a further increase of approximately 28% is experienced, yielding 17 events per season. Flagstaff, AZ, shows an even larger change in frequency when the summer mean maximum (Tx) delta is applied, with the baseline once-per-year extreme heat event occurring 18 times per summer in the future.

Table 2. Recurrence Analysis for Baltimore, MD, and Flagstaff, AZ[a]

	Baseline (1971–2000)	2051–2069 Using Mean Changes	2051–2069 Using Extreme Changes
Baltimore, MD (JJA maximum)	Current once-per-year event: 99°F	The current event is met or exceeded 13.1 times per year	The current event is met or exceeded 16.8 times per year
Baltimore, MD (DJF minimum)	Current once-per-year event: 3°F	Values below the current level occur 0.3 times per year	Values below the current level occur 0.1 times per year
Flagstaff, AZ (JJA maximum)	Current once-per-year: event 92°F	The current event is met or exceeded 17.5 times per year	The current event is met or exceeded 17.5 times per year
Flagstaff, AZ (DJF minimum)	Current once-per-year event: −9°F	Values below the current level occur 0.5 times per year	Values below the current level occur 0.4 times per year

[a]Observed weather data for Baltimore and Flagstaff were obtained from the National Climatic Data Center (NCDC) Global Historical Climatology Network (GHCN) [*Lawrimore et al.*, 2011].

However, because TXx and Tx in the southwest domain are nearly identical (unlike the northeast case), the frequency of occurrence (18 times per summer) is the same when either delta is applied. While the precise numbers should not be emphasized, the magnitude of the changes suggests the potential for large societal challenges (for example, see the *Petkova et al.* [2013] analysis of heat-related mortality in northeastern cities), even in the absence of nonlinear impacts associated with high temperatures. In Baltimore, applying a Tn delta turns the current once-per-year cold extreme into a roughly 1 in 4 year event in the 2050s, whereas applying the delta change associated with TNn in the models yields a recurrence of only once per 10 years. An order of magnitude decrease in the frequency of extreme cold events would produce a range of impacts, including greater survivability of overwintering pests [*Porter et al.*, 1991].

5. Discussion/Conclusions

Using regional climate models, we report that summertime extreme maximum temperatures are projected to increase more than summertime mean daily maximum temperatures over much of the eastern U.S. It should be noted that in some regions, the annual maximum temperature may not occur in JJA; close to the Pacific coast, it is common for TXx to occur after JJA, due to warming sea surface temperatures and frequent easterly descending winds [*NCDC*, 2014a]. Our DJF emphasis generally successfully captures the coldest day per year over the entire contiguous U.S. [*NCDC*, 2014b]. Changes in wintertime extreme minimum temperatures are appreciably larger than changes in the wintertime mean minimum, with a few exceptions largely confined to the southernmost U.S. We demonstrate that application of projected changes associated with the extremes of the distribution to historical station data leads to large changes in extreme event frequency. For example, Baltimore's high-temperature extreme that was met or exceeded once per year historically is projected to occur as many as 17 times per season by midcentury, a 28% increase relative to projections based on the mean daily maximum temperature change. The same approach projects that the historical once-per-year cold event in Baltimore will become a once-per-decade event by midcentury.

We show that the NARCCAP models are able to reproduce the dynamical patterns as expressed in the 500 hPa geopotential height field associated with extreme temperatures in the two subregions. We also show that projected future changes in these extreme events in NARCCAP cannot be explained by geopotential height anomalies or lower boundary conditions as reflected by soil moisture in summer and snow water equivalent in winter.

While the 50 km^2 resolution of NARCCAP is an improvement over GCMs, it remains too coarse to resolve important fine-scale features that could influence differential temperature changes as the globe warms, such as land-sea contrasts, variations in topography, and urban heat islands. Further, while this study focused on one threshold for extreme temperatures, other studies have noted that the use of different thresholds can yield different results, both for observations and projections [*Seneviratne et al.*, 2012]. The results shown here are also constrained to the few GCM and RCM pairings (and the absence of multiple ensemble members) available through NARCCAP. Future work will use the broader Coupled Model Intercomparison Project Phase 5 (CMIP5) GCM ensemble [e.g., *Thibeault and Seth*, 2014], which includes several models that are beginning to approach the spatial resolution of NARCCAP, to explore how dynamical changes and soil moisture anomalies may combine to influence extreme heat events. To address this question, it will be important to look at larger numbers of days in models and observations, including sequences of hot days, in order to explore, for example, the evolution of soil moisture anomalies during heat events. However, even the full set of CMIP5 models and ensemble members may not characterize all extreme temperature event outcomes, especially to the extent that GCM projections may underestimate possible drivers of changes in midlatitude temperature extremes such as declining Arctic sea ice [*Liu et al.*, 2012, 2013] and aerosols.

Acknowledgments
This work was supported by the Department of the Interior Northeast Climate Science Center and the NOAA-RISA Program through the Consortium for Climate Risk in the Urban Northeast. We acknowledge the regional climate modeling groups, North American Regional Climate Change Assessment Program [*Mearns and Gutowski*, 2009]. We also acknowledge the global climate modeling groups, the Program for Climate Model Diagnosis, and Intercomparison (PCMDI) and the WCRP for the CMIP3 multimodel data set, supported by the Office of Science, U.S. Department of Energy.

The Editor thanks two anonymous reviewers for their assistance in evaluating this paper.

References

Ahmed, K. F., G. Wang, J. Silander, A. M. Wilson, J. M. Allen, R. Horton, and R. Anyah (2013), Statistical downscaling and bias correction of climate model outputs for climate change impact assessment in the U.S. northeast, *Global Planet. Change*, *100*, 320–332, doi:10.1016/j.gloplacha.2012.11.003.

Alexander, L. V., et al. (2006), Global observed changes in daily climate extremes of temperature and precipitation, *J. Geophys. Res.*, *111*, D05109, doi:10.1029/2005JD006290.

Ammunét, T., T. Kaukoranta, K. Saikkonen, T. Repo, and T. Klemola (2012), Invading and resident defoliators in a changing climate: Cold tolerance and predictions concerning extreme winter cold as a range-limiting factor, *Ecol. Entomol.*, *37*(3), 212–220, doi:10.1111/j.1365-2311.2012.01358.x.

Ballester, J., X. Rodó, and F. Giorgi (2009), Future changes in Central Europe heat waves expected to mostly follow summer mean warming, *Clim. Dyn.*, *35*(7–8), 1191–1205, doi:10.1007/s00382-009-0641-5.

Bradbury, J. A., B. D. Keim, and C. P. Wake (2002), U.S. East Coast trough indices at 500 hPa and New England winter climate variability, *J. Clim.*, *15*(23), 3509–3517, doi:10.1175/1520-0442(2002)015<3509:USECTI>2.0.CO;2.

Bukovsky, M. S. (2012), Temperature trends in the NARCCAP regional climate models, *J. Clim.*, *25*(11), 3985–3991, doi:10.1175/JCLI-D-11-00588.1.

Bukovsky, M. S., D. J. Gochis, and L. O. Mearns (2013), Towards assessing NARCCAP regional climate model credibility for the North American Monsoon: Current climate simulations*, *J. Clim.*, *26*(22), 8802–8826, doi:10.1175/JCLI-D-12-00538.1.

Caldwell, P., H.-N. S. Chin, D. C. Bader, and G. Bala (2009), Evaluation of a WRF dynamical downscaling simulation over California, *Clim. Change*, *95*(3–4), 499–521, doi:10.1007/s10584-009-9583-5.

Coffel, E., and R. Horton (2015), Climate change and the impact of extreme temperatures on aviation, *Weather Clim. Soc.*, *7*(Anderson 1999), 94–102, doi:10.1175/WCAS-D-14-00026.1.

Cook, B. I., T. R. Ault, and J. E. Smerdon (2015), Unprecedented 21st century drought risk in the American Southwest and Central Plains, *Sci. Adv.*, *February*, 1–7, doi:10.1126/sciadv.1400082.

Diffenbaugh, N. S., and M. Ashfaq (2010), Intensification of hot extremes in the United States, *Geophys. Res. Lett.*, *37*, L15701, doi:10.1029/2010GL043888.

Diffenbaugh, N. S., J. S. Pal, R. J. Trapp, and F. Giorgi (2005), Fine-scale processes regulate the response of extreme events to global climate change, *Proc. Natl. Acad. Sci.*, *102*(44), 15,774–15,778, doi:10.1073/pnas.0506042102.

Ellis, A. W., and D. J. Leathers (1999), Analysis of cold airmass temperature modification across the U.S. Great Plains as a consequence of snow depth and Albedo, *J. Appl. Meteorol.*, *38*(6), 696–711, doi:10.1175/1520-0450(1999)038<0696:AOCATM>2.0.CO;2.

Handmer, J., et al. (2012), Changes in impacts of climate extremes: Human systems and ecosystems, in *Managing the Risks of Extreme Events and Disasters to Advance Climate Change Adaptation*, edited by C. Field et al., pp. 231–290, A Special Report of Working Groups I and II of the Intergovernmental Panel on Climate Change: Managing the Risks of Extreme Events and Disasters to Advance Climate Change Adaptation, Cambridge Univ. Press, Cambridge, U. K., and New York.

Hartmann, D., et al. (2013), Observations: Atmosphere and surface, in *Climate Change 2013: The Physical Science Basis. Contribution of Working Group I to the Fifth Assessment Report of the Intergovernmental Panel on Climate Change*, edited by T. Stocker et al., pp. 159–254, Cambridge Univ. Press, Cambridge, U. K., and New York.

Hirschi, M., S. I. Seneviratne, V. Alexandrov, F. Boberg, C. Boroneant, O. B. Christensen, H. Formayer, B. Orlowsky, and P. Stepanek (2010), Observational evidence for soil-moisture impact on hot extremes in southeastern Europe, *Nat. Geosci.*, *4*(1), 17–21, doi:10.1038/ngeo1032.

Horton, R., C. Rosenzweig, V. Gornitz, D. Bader, and M. O'Grady (2010), Climate risk information, *Ann. N.Y. Acad. Sci.*, *1196*, 147–228.

Jones, B., B. C. O'Neill, L. McDaniel, S. McGinnis, L. O. Mearns, and C. Tebaldi (2015), Future population exposure to U.S. heat extremes, *Nat. Clim. Change*, *5*, 652–655, doi:10.1038/nclimate2631.

Kalkstein, L. S., and J. S. Greene (1997), An evaluation of climate/mortality relationships in large U.S. cities and the possible impacts of a climate change, *Environ. Health Perspect.*, *105*(1), 84–93, doi:10.1289/ehp.9710584.

Kharin, V. V., F. W. Zwiers, X. Zhang, and G. C. Hegerl (2007), Changes in temperature and precipitation extremes in the IPCC ensemble of global coupled model simulations, *J. Clim.*, *20*(8), 1419–1444, doi:10.1175/JCLI4066.1.

Kjellström, E., L. Bärring, D. Jacob, R. Jones, G. Lenderink, and C. Schär (2007), Modelling daily temperature extremes: Recent climate and future changes over Europe, *Clim. Change*, *81*(S1), 249–265, doi:10.1007/s10584-006-9220-5.

Kunkel, K. E., X.-Z. Liang, J. Zhu, and Y. Lin (2006), Can CGCMs simulate the twentieth-century "Warming Hole" in the central United States?, *J. Clim.*, *19*(17), 4137–4153, doi:10.1175/JCLI3848.1.

Lawrimore, J. H., M. J. Menne, B. E. Gleason, C. N. Williams, D. B. Wuertz, R. S. Vose, and J. Rennie (2011), An overview of the Global Historical Climatology Network monthly mean temperature data set, version 3, *J. Geophys. Res.*, *116*, D19121, doi:10.1029/2011JD016187.

Leathers, D. J., A. W. Ellis, and D. A. Robinson (1995), Characteristics of temperature depressions associated with snow cover across the northeast United States, *J. Appl. Meteorol.*, *34*, 381–390.

Liu, J., J. Curry, H. Wang, M. Song, and R. M. Horton (2012), Impact of declining Arctic sea ice on winter snowfall, *Proc. Natl. Acad. Sci.*, *109*(11), 4074–4079.

Liu, J., M. Song, R. M. Horton, and Y. Hu (2013), Reducing spread in climate model projections of a September ice-free Arctic, *Proc. Natl. Acad. Sci. U.S.A.*, *110*(31), 12,571–12,576, doi:10.1073/pnas.1219716110.

Mearns, L., and W. Gutowski (2009), A regional climate change assessment program for North America, *EOS Trans.*, *90*(36), 2008–2009.

Mearns, L. O., et al. (2012), The North American regional climate change assessment program: Overview of phase I results, *Bull. Am. Meteorol. Soc.*, *93*(9), 1337–1362, doi:10.1175/BAMS-D-11-00223.1.

Mearns, L. O., D. P. Lettenmaier, and S. McGinnis (2015), Uses of results of regional climate model experiments for impacts and adaptation studies: The example of NARCCAP, *Curr. Clim. Change Rep.*, *1*, 1–9, doi:10.1007/s40641-015-0004-8.

Meehl, G. a., and C. Tebaldi (2004), More intense, more frequent, and longer lasting heat waves in the 21st century, *Science*, *305*(5686), 994–997, doi:10.1126/science.1098704.

Meehl, G. A., C. Tebaldi, G. Walton, D. Easterling, and L. McDaniel (2009), Relative increase of record high maximum temperatures compared to record low minimum temperatures in the U.S., *Geophys. Res. Lett.*, *36*, L23701, doi:10.1029/2009GL040736.

Meehl, G. A., J. M. Arblaster, and G. Branstator (2012), Mechanisms contributing to the warming hole and the consequent U.S. East-West differential of heat extremes, *J. Clim.*, *25*(18), 6394–6408, doi:10.1175/JCLI-D-11-00655.1.

Mesinger, F., et al. (2006), North American regional reanalysis, *Bull. Am. Meteorol. Soc.*, *87*(3), 343–360, doi:10.1175/BAMS-87-3-343.

Meyer, M., A. Amekudzi, and J. O'Har (2010), Transportation asset management systems and climate change, *Trans. Res. Record*, *2160*(-1), 12–20, doi:10.3141/2160-02.

Nakicenovic, N., et al. (2000), *Special Report on Emissions Scenarios*, Cambridge Univ. Press, Cambridge, U. K.

NCDC, N. (2014a), Mercury rising: When to expect the "Warmest Day of the Year". National Climatic Data Center (NCDC). [Available at http: //www.ncdc.noaa.gov/news/mercury-rising-when-expect-warmest-day-year, Accessed on June 16, 2015.]

NCDC, N. (2014b), When to expect the "Coldest Day of the Year". [Available at https://www.ncdc.noaa.gov/news/when-to-expect-coldest-day-of-year, Accessed on June 16, 2015.]

Ning, L., and R. S. Bradley (2015), Winter climate extremes over the northeastern United States and southeastern Canada and teleconnections with large-scale modes of climate variability*, *J. Clim.*, *28*(6), 2475–2493, doi:10.1175/JCLI-D-13-00750.1.

Ning, L., E. E. Riddle, and R. S. Bradley (2015), Projected changes in climate extremes over the northeastern United States*, *J. Clim.*, *28*(8), 3289–3310, doi:10.1175/JCLI-D-14-00150.1.

National Oceanic and Atmospheric Administration (2015), U.S. weather related fatalities. [Available at http://www.nws.noaa.gov/om/hazstats.shtml, Accessed on June 16, 2015.]

Orlowsky, B., and S. I. Seneviratne (2011), Global changes in extreme events: Regional and seasonal dimension, *Clim. Change*, *110*(3–4), 669–696, doi:10.1007/s10584-011-0122-9.

Pan, Z., R. W. Arritt, E. S. Takle, W. J. Gutowski, C. J. Anderson, and M. Segal (2004), Altered hydrologic feedback in a warming climate introduces a "warming hole", *Geophys. Res. Lett.*, *31*, L17109, doi:10.1029/2004GL020528.

Petkova, E. P., R. M. Horton, D. a. Bader, and P. L. Kinney (2013), Projected heat-related mortality in the U.S. urban northeast, *Int. J. Environ. Res. Publ. Health*, *10*, 6734–6747, doi:10.3390/ijerph10126734.

Porter, J. H., M. L. Parry, and T. R. Carter (1991), The potential effects of climatic change on agricultural insect pests, *Agric. Forest Meteorol.*, *57*, 221–240, doi:10.1016/0168-1923(91)90088-8.

Sathaye, J. A., L. L. Dale, P. H. Larsen, G. A. Fitts, K. Koy, S. M. Lewis, and A. F. P. de Lucena (2013), Estimating impacts of warming temperatures on California's electricity system, *Global Environ. Change*, *23*(2), 499–511, doi:10.1016/j.gloenvcha.2012.12.005.

Schär, C., P. L. Vidale, D. Lüthi, C. Frei, C. Häberli, M. A. Liniger, and C. Appenzeller (2004), The role of increasing temperature variability in European summer heatwaves, *Nature*, *427*(6972), 332–336, doi:10.1038/nature02300.

Schlenker, W., and M. J. Roberts (2009), Nonlinear temperature effects indicate severe damages to U.S. crop yields under climate change, *Proc. Natl. Acad. Sci.*, *106*(37), 15,594–15,598, doi:10.1073/pnas.0906865106.

Seneviratne, S., et al. (2012), Changes in climate extremes and their impacts on the natural physical environment, in *A Special Report of Working Groups I and II of the Intergovernmental Panel on Climate Change: Managing the Risks of Extreme Events and Disasters to Advance Climate Change Adaptation*, edited by C. Field et al., Cambridge Univ. Press, Cambridge, U. K., and New York.

Sobolowski, S., and T. Pavelsky (2012), Evaluation of present and future North American Regional Climate Change Assessment Program (NARCCAP) regional climate simulations over the southeast United States, *J. Geophys. Res.*, *117*, D01101, doi:10.1029/2011JD016430.

Thibeault, J. M., and A. Seth (2014), Changing climate extremes in the Northeast United States: Observations and projections from CMIP5, *Clim. Change*, *127*, 273–287, doi:10.1007/s10584-014-1257-2.

Walsh, J., et al. (2014), Ch. 2: Our changing climate, in *Climate Change Impacts in the United States: The Third National Climate Assessment*, edited by J. Walsh et al., pp. 19–67, U.S. Global Change Research Program, Washington, D. C.

Yarnal, B., and D. J. Leathers (1988), Relationships between interdecadal and interannual climatic variations and their effect on Pennsylvania climate, *Ann. Assoc. Am. Geogr.*, *78*(4), 624–641, doi:10.1111/j.1467-8306.1988.tb00235.x.